ELSEVIER

Biophysical Chemistry 68 (1997) 63–72

Biophysical Chemistry

Imaging and nano-manipulation of single biomolecules

Takashi Funatsu [a,*], Yoshie Harada [a], Hideo Higuchi [a], Makio Tokunaga [a], Kiwamu Saito [a], Yoshiharu Ishii [a], Ronald D. Vale [a,b,c], Toshio Yanagida [a,d,e]

[a] *Yanagida Biomotron Project, ERATO, JST, Senba-Higashi 2-4-14, Mino, Osaka 562, Japan*
[b] *Howard Hughes Medical Institute, University of California, San Francisco, CA 94143, USA*
[c] *Department of Pharmacology, University of California, San Francisco, CA 94143, USA*
[d] *Department of Biophysical Engineering, Osaka University, Toyonaka, Osaka 560, Japan*
[e] *Department of Physiology, Osaka University Medical School, Suita, Osaka 565, Japan*

Received 16 December 1996; accepted 16 January 1997

Abstract

We have developed a new technique for imaging single fluorescent dye molecules by refining epifluorescence and total internal reflection fluorescence microscopies. In contrast to previously reported single fluorescent molecule imaging methods, in which specimens were immobilized on an air-dried surface, our method enables video-rate imaging of single molecules in aqueous solution. This approach enabled us to directly image the processive movement of individual fluorescently labeled kinesin molecules along a microtubule. This method was also used to visualize individual ATP turnover reactions of single myosin molecules. The method can be combined with molecular manipulation using an optical trap. A single kinesin molecule attached to a polystyrene bead was brought into contact with a microtubule adsorbed onto the glass surface. The lifetime of bound Cy3-nucleotide in the absence or presence of the microtubule was 10 s or 0.08 s, respectively, showing that ATPase activity of the kinesin is strongly activated by microtubules. As the present system is equipped with a nanometer sensor, elemental steps of a single kinesin molecule can also be measured. By simultaneously measuring the individual ATP turnovers and elementary mechanical events of a single kinesin molecule, we will be able to obtain a clear answer to the fundamental problem of how the mechanical events are coupled to the ATPase reaction. © 1997 Elsevier Science B.V.

Keywords: Single-molecule imaging; Motor protein; ATPase; Fluorescence microscopy

1. Introduction

The function of biomolecules has traditionally been studied by using a solution containing more than 10^{10} molecules. All we can obtain there is the average values of the huge number of molecules and this situation sometimes makes it difficult to interpret the data. The best way to obtain unambiguous

Abbreviations: TIRFM, total internal reflection fluorescence microscopy; HMM, heavy meromyosin; S1, myosin subfragment 1

* Corresponding author. Fax: 81-727-28-7033; tel: 81-727-28-7003; e-mail: funatsu@yanagida.jstc.go.jp

PII S0301-4622(97)00008-2

information about the function of biomolecules is to study their function at the level of single molecules. Imaging and manipulation of individual molecules under an optical microscope are promising for understanding the working principle of biomolecular machines such as molecular motors. Due to the diffraction limit of the light, however, the resolution of the conventional microscope ($\sim 0.2\ \mu m$) is too low to observe single protein molecules.

Fluorescence microscopy is useful when observing objects smaller than the diffraction limit. By observing the fluorescence from a single molecule, we can detect its presence. About ten years ago, it was demonstrated that single actin filaments (double helical polymer of actin), labeled with fluorescent phalloidin, can be clearly seen by fluorescence microscopy [1]. This finding led to the development of new *in vitro* motility assays that address the elementary process of force generation by acto–myosin interaction directly at the molecular level [2–5]. More recently, combining actin filament manipulation techniques with nanometry, unitary forces and steps driven by ATP hydrolysis have been directly recorded at very high resolution from multiple [6] and single myosin molecules [7,8]. In this case, actin filaments were visualized with hundreds of fluorophores and individual myosin could not be visualized. Thus, the next step would be imaging of single fluorescent molecules, which allow visualization of the function of biomolecules such as motor protein.

Single fluorescent dye molecules, excited by a relatively strong light source such as a laser under a conventional microscope, emit enough photons to be visualized with a commercial high sensitivity video camera [9]. However, imaging single fluorescent dye molecules in solution requires extracting the signal from a huge background of scattering and luminescence. Betzig and his colleagues succeeded in imaging single fluorescent dye molecules at an air–surface interface by reducing the optical excitation volume to subwavelength proportions using illumination mode near-field scanning optical microscopy [10,11]. This method, however, is difficult to apply to real time imaging of single protein molecules undergoing motions and ATPase reaction in aqueous solution, because the field image is acquired by scanning with a sharp optical probe for several minutes.

We have recently developed fluorescence microscopes which have 50 to > 2000-fold smaller background noise than a conventional fluorescence microscope and thus permit the visualization of single fluorescent dye molecules in aqueous solution [12]. Here, we demonstrate that the movements and individual ATP turnovers of single motor proteins can be directly visualized at video-rate.

2. Materials and methods

2.1. Visualization of single fluorescent dye molecules in aqueous solution

2.1.1. Low background epifluorescence microscopy

An inverted microscope equipped with epifluorescence optics (TMD300, Nikon Inc., Japan) was modified as follows (Fig. 1). A beam of an Ar laser (514.5 nm; LEXEL MODEL 95; Cooper Laser Sonic, USA) or a He–Ne laser (633 nm; GLG5740; NEC, Japan) was depolarized by passing through a quarter-wave plate and focused on a rotating ground glass. The beam was passed through a pinhole and was collimated with a lens ($f = 40$ mm). The beam was focused on an aperture diaphragm and was introduced into the objective lens (NCF Plan Apo × 100; NA 1.4; Nikon, Japan) through a quartz dichroic mirror (Sigma Koki, Japan). The specimens were

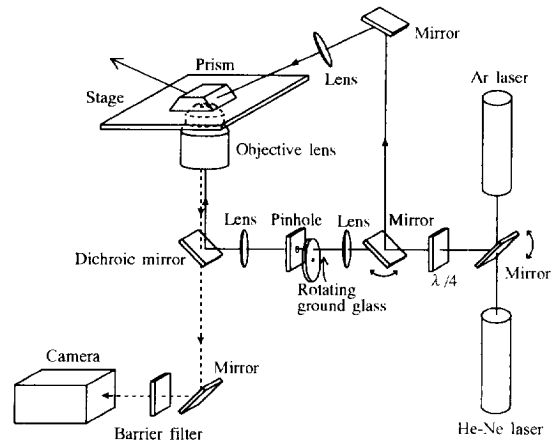

Fig. 1. Schematic drawing of the optical system for single fluorophore imaging (see materials and methods for details). An inverted microscope equipped with epifluorescence was modified to reduce background luminescence. To reduce the background further, total internal reflection optics were installed.

excited by paraxial rays with Koehler illumination. All glass optical parts, except for the objective lens, were replaced with ones made of fused silica, which emits little fluorescence. Fluorescence-free silicon oil ($n = 1.51$; 70% (v/v) of KF-56 and 30% (v/v) of F-4; Shinetsu Silicon, Japan) was used as immersion oil. Background luminescence was rejected with a barrier filter (570DF30 for the Ar laser and 670DF40 for the He–Ne laser; Omega Optical, USA). To reduce dust contamination, quartz slides were washed with 0.1 M KOH and ethanol. Dust in solution was removed by filtration (pore size 0.2 μm). Experiments were performed in a class 1000 clean room.

2.1.2. Total internal reflection fluorescence microscopy (TIRFM)

The total internal reflection optics were installed on the inverted microscope (Fig. 1) [13]. The laser beam was incident on a quartz microscope slide through a quartz prism. The gap between the microscope slide and the prism was filled with fluorescence-free pure glycerol. The incident angle at the quartz slide-to-solution was 68° to the normal (the critical angle was 65.5°). The beam was focused by a lens to a cross-section of 100 μm × 200 μm at the specimen plane.

2.1.3. Imaging and analysis

For observation of movement or changes in fluorescence intensity, images were taken by a CCD (C2400-77, Hamamatsu Photonics, Japan) or a SIT camera (C2400-08, Hamamatsu Photonics, Japan) coupled to an image intensifier (C2400-80H, Hamamatsu Photonics, Japan). The images were quantified from the video tape recorder using a computer image processor (Avio Excel, Nippon Avionics, Japan). A cooled CCD camera (series 4200; Astromed, UK) was used for quantitative analysis with low temporal resolution.

2.1.4. Preparation of Cy3-labeled heavy meromyosin (HMM)

Actin and heavy meromyosin (HMM) were prepared from skeletal muscle as described previously [1]. SH-1 of myosin heads were labeled to a stoichiometry of 0.7 dyes per polypeptide with Cy3-maleimide obtained by linking Cy3.18-OSu (Amersham Life Science, USA) [14] to *N*-(2-(1-piperazinyl)ethyl) maleimide (Dojindo Laboratories, Japan).

2.2. Direct observation of single kinesin molecules moving along microtubules

2.2.1. Preparation of Cy3-labeled kinesin and Cy5-labeled axonemes

The ubiquitous human kinesin gene [15] was truncated just before the hinge at amino-acid residue 560 and a short peptide containing a reactive cysteine (PSIVHRKCF) [16] was introduced at the C terminus (uhK560cys). uhK560cys was expressed in *Escherichia coli*, purified, and reacted at its C-terminus cysteine with a Cy3-maleimide at a stoichiometry of 0.1–0.5 dyes per polypeptide chain. Axonemes were prepared from *Chlamydomonas* [17] and labeled with Cy5.18-Osu (Amersham Life Science, USA) [14].

2.2.2. Single fluorescence assay of the movement of kinesin

Cy5-labeled axonemes were mixed with 0.5–1.5 nM uhk560-Cy3 in a solution containing 12 mM PIPES (pH 6.8), 2 mM $MgCl_2$, 1 mM EGTA, 1 mM ATP, 7.5 mg ml^{-1} BSA, 0.5% 2-mercaptoethanol and an oxygen scavenger system [18] at 25°C. Movement of uhK560-Cy3 on axoneme was observed by TIRFM.

2.3. Direct observation of individual ATP turnovers by single myosin molecules

2.3.1. Preparation of Cy5-labeled S1 and Cy3-ATP

Cy5-maleimide was obtained by linking Cy5.18-OSu (Amersham Life Science, USA) to *N*-(2-(1-piperazinyl)ethyl) maleimide (Dojindo Laboratories, Japan). Cysteine residues of myosin regulatory light chains were labeled with Cy5-maleimide and exchanged into S-1 [19]. Cy3-ATP was prepared by coupling of Cy3.29-Osu (Amersham Life Science, USA) with N^6-((6-aminohexyl)carbamoylmethyl)-ATP [20].

2.3.2. Measurement of ATPase activity of S1 suspended in solution

Mg-ATPase activity of S-1 suspended in solution was determined by measuring the Pi release rate [21]. The dissociation rate of bound Cy3-nucleotide (ATP

or ADP) from S-1 was obtained from the ATPase rate at saturated concentration of Cy3-ATP (15 μM), in which the ATPase rate is approximately equal to the dissociation rate.

2.3.3. Measurement of Cy3-ATP turnover of S1 with single fluorescence imaging

S-1 molecules, whose regulatory light chains were labeled with Cy5, were adsorbed onto the quartz slide surface and their positions were visualized. The ATP turnover events were detected by directly observing association–(hydrolysis)–dissociation of Cy3-ATP corresponding to the position of Cy5-S-1 molecules on the surface. Experiments were performed in a buffer containing 10 nM Cy3-ATP, 25 mM KCl, 3 mM $MgCl_2$, 20 mM HEPES (pH 7.8), 0.5% 2-mercaptoethanol and an oxygen scavenger system [18] at 25°C.

2.4. Individual ATP turnovers by single kinesin molecules captured by optical tweezers

2.4.1. Apparatus for laser tweezers and nanometry

The optical trap was installed onto an inverted fluorescence microscope for imaging of single fluorophores. A diode pumped Nd:YAG laser (1064 nm; 7910-Y4-106, Spectra Physics, USA) and an objective lens (Plan NCF Fluor × 100, Nikon, Japan) were used. The transmitted bright-field image of the bead, illuminated by infrared light (750–900 nm) from a halogen lamp, was projected onto a quadrant photodiode (s944-13, Hamamatsu Photonics, Japan). Nanometer displacement of the beads were determined from the differential outputs of a quadrant photodiode detector. The trapping stiffness (0.05 pN nm^{-1}) was determined from the thermal fluctuation of the beads using the equipartition law [22]. Data were filtered by a low pass filter having a 10 Hz cutoff frequency. An avalanche photodiode (SPCM-200-PQ, EG and G Optoelectronics, Canada) was placed at an image plane and photon currents from Cy3-ATP were counted. Data of displacement and fluorescence intensity of Cy3-ATP were simultaneously recorded by microcomputer.

2.4.2. Preparation of kinesin-coated beads, Cy5-labeled microtubule, and Cy3-ATP

Kinesin was purified from bovine brain by microtubule affinity followed by DEAE chromatography (Fractogel DEAE, Merck) and sedimentation [23]. Kinesin was attached to a bead of 1 μm diameter according to the method of Svoboda and colleagues [22,24]. Tubulin was prepared from bovine brain and labeled with Cy5.18-Osu [25,26]. Microtubules were prepared by copolymerization of fluorescent and nonfluorescent tubulin in a molar ratio of 1 to 4 and stabilized by 10 μM taxol. Ribose-linked Cy3-ATP was prepared by reaction of 2′(3′)-*O*-[(aminoethyl)carbamoyl]adenosine 5′-triphosphate with Cy3.29-Osu [27,28].

3. Results and discussion

3.1. Visualization of single fluorescent dye molecules in aqueous solution

The number of photons emitted from a single fluorophore when excited by a strong light source of a laser is sufficient to be visualized by a commercial sensitive video camera. The problem is that background luminescence and Raman scattering by water are huge in a conventional fluorescence microscope. The background luminescence is > 10-fold larger than the fluorescence from a single fluorophore (Fig. 2). Therefore, the key point for imaging single fluorescent molecules is how to eliminate the background. By reducing the background luminescence of an epifluorescence microscope, single fluorescent dye molecules can be visualized [12,29].

Evidence that single fluorescent dye molecules

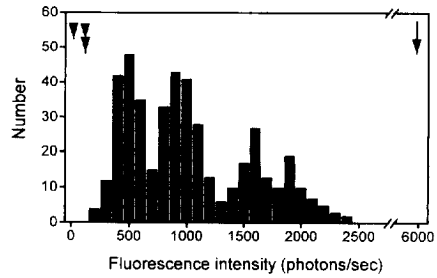

Fig. 2. Histogram of fluorescence intensity from Cy3-labeled HMMs. The laser power was 10 mW at the objective plane and the illumination area was 150 μm in diameter. Images were taken with a cooled CCD camera at 5 s exposure. The single and double arrow heads indicate the background in TIRFM and low background epifluorescence microscopy, respectively. The arrow indicates the background before refinement.

bound to HMM could be seen was obtained in three different ways. The fluorescent dye Cy3 was bound specifically to a reactive thiol group (SH-1) on each head of HMM (HMM has two heads) at an average dye to head molar ratio of 0.7:1. Therefore, the average molar ratio of HMM with two, one and no bound Cy3 molecules would be approximately 5:4:1. Fluorescence images of Cy3-HMM spread on the surface of a coverslip at very low density (< 0.13 HMMs μm^{-2}) appeared as bright spots (e.g., Fig. 4A). Fig. 2 shows the histogram of intensities of individual fluorescent spots. Fluorescent spot intensities were quantized at intervals of approximately 500 photons s^{-1}. Fluorescence intensities of more than 1500 photons s^{-1} very likely result from two HMM molecules that were located in close proximity. When the incident light power was increased 10-fold, the fluorescent spots became substantially brighter but the number of spots observed was unchanged, indicating that the intensity of 500 photons s^{-1} is the minimum quantity, i.e., due to single fluorescent dye molecules (1st evidence). Furthermore, we confirmed that the least intense spots corresponding to the minimum quantity were bleached in a single step, while the next most intense spots were bleached in two steps (2nd evidence). Such stepwise photobleaching was most clearly observed with the second imaging method described below (Fig. 4B). Finally, we show that the spots observed by fluorescence microscopy correspond to individual HMM molecules by electron microscopy. Fig. 3A shows fluorescence images of Cy3-HMM molecules. Fig. 3B shows the electron micrograph of the same field as that shown in Fig. 3A. Single HMM molecules,

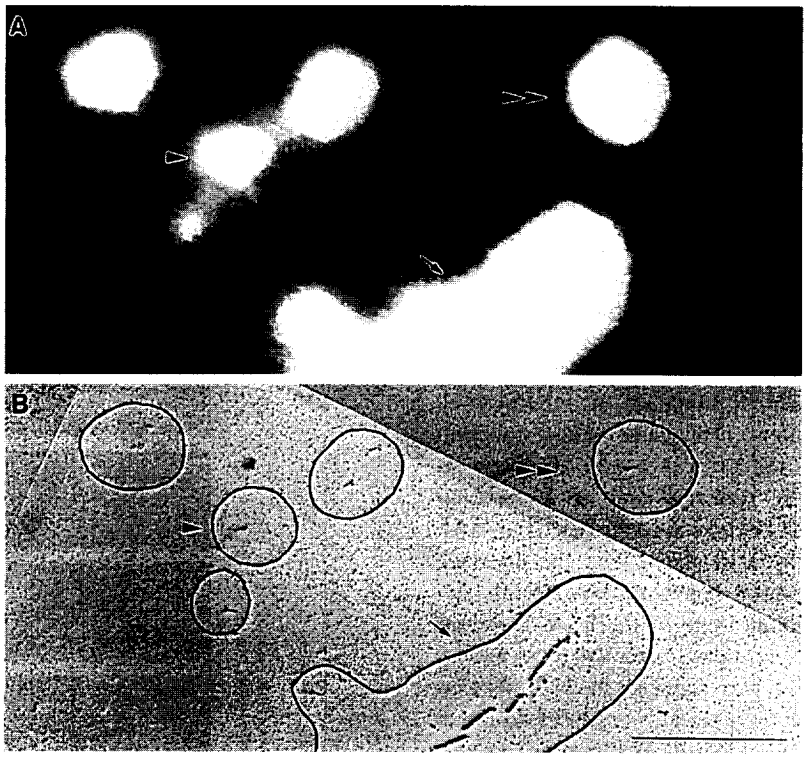

Fig. 3. Low background epifluorescence microscopy imaging. (A) Fluorescence micrograph taken by low background epifluorescence microscopy. Cy3-labeled HMMs were spread on a mica film to enable subsequent electron microscopy. The fluorescence images were obtained by averaging 64 frames of the video. As a marker to identify position, phalloidin tetramethyl rhodamine-labeled actin filaments were included (shown by arrow). The typical fluorescence spots due to one and two fluorophores are indicated by single and double arrow heads, respectively. (B) Rotary-shadowed electron micrograph of the same field and magnification as in (A). The outlines of the fluorescence images are shown by solid lines. Scale bar = 1 μm.

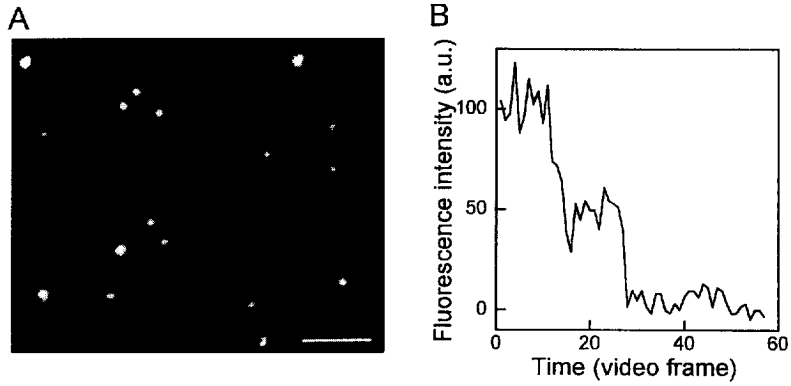

Fig. 4. Low background total internal reflection fluorescence microscopy imaging. (A) A micrograph of Cy3-labeled HMM molecules taken at one frame of the video (exposure time 1/30 s). Single and double arrowheads indicate typical fluorescence spots due to one and two dye molecules bound to HMM. (B) Quantized photobleaching of fluorescent molecules observed at the video rate (1/30 s); a.u. = arbitrary units.

identified by their characteristic two-headed shape, were found in positions (single arrow heads) corresponding to the least intense fluorescent spots (the first Gaussian peak in Fig. 2), or in positions (double arrow heads) of more intense fluorescent spots (the second Gaussian peak in Fig. 2). Thus the least intense fluorescent spots are due to single fluorescent molecules attached to one of the two heads of HMM (3rd evidence). Taken together, the evidence described above provides strong support that single fluorescent molecules can be visualized.

In order to further decrease the background luminescence, we reduced the optical excitation volume, using evanescent-field illumination of TIRFM [12]. When a laser is incident on a quartz slide-to-medium interface at above the critical angle, the light is totally and internally reflected and an evanescent field is produced just beyond the interface (Fig. 6A). This evanescent field is localized near the interface with the $1/e$ penetration depth of 100–200 nm, depending on the incident angle of the laser. Combining the low background optics with the local excitation, the background was reduced to 1–3 photons s^{-1} per diffraction limit area, i.e. > 2000-fold lower than that for a conventional epifluorescence microscope. Thus, single fluorophores bound to HMM molecules could be clearly visualized at a full-video rate (1/30 s) without frame averaging (Fig. 4). The time course of stepwise photobleaching from two dye molecules was clearly observed.

3.2. Direct observation of single kinesin molecules moving along microtubules

We applied low-background TIRFM to observe processive movement of individual fluorescently labeled kinesin molecules along a microtubule [30]. To

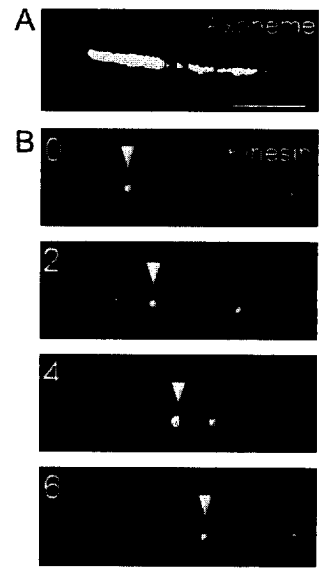

Fig. 5. Movement of single fluorescently labeled kinesin molecules along an axoneme. (A) A micrograph of Cy5-labeled axoneme. (B) Micrographs of Cy3-labeled kinesin. Arrowheads track a moving fluorescence spot of kinesin. Times at which micrographs were taken are indicated in each panel. Scale bar = 5 μm.

fluorescently label kinesin without losing the motor function, the ubiquitous kinesin gene was truncated at amino-acid residue 560 and a short peptide containing a highly reactive cysteine was introduced at the C-terminus (uhK560cys). It was expressed in *Escherichia coli*, purified, and labeled with Cy3-maleimide.

uhK560-Cy3 (0.6 nM) was applied to Cy5-labeled flagellar axonemes adsorbed on the surface of a quartz slide and observed by TIRFM. uhK560-Cy3 that associated with the axoneme could be seen as clear, in-focus spots, whereas those undergoing Brownian motion moved too rapidly to be seen as discrete spots. uhK560-Cy3 could been seen moving unidirectionally along axonemal microtubules (Fig. 5). The velocity of movement was 0.3 $\mu m\,s^{-1}$, which was similar to the gliding velocity of an axoneme moving over a glass surface coated with uhK560-Cy3. The distance travelled by uhK560-Cy3 was distributed exponentially [30,31] with a mean distance of 0.63 μm. Based upon the mean travel distance of 630 nm and an 8 nm step per mechanical cycle of kinesin, the probability of remaining bound to the microtubule per mechanical cycle is $\sim 99\%$.

3.3. Direct observation of individual ATP turnovers by single myosin molecules

Local illumination of TIRFM enabled us to detect individual Mg-ATP turnovers by single S-1 (myosin subfragment 1) molecules. S-1 molecules labeled with Cy5 were adsorbed onto the quartz slide surface and their positions were marked. The ATP turnover events were detected by directly observing association–(hydrolysis)–dissociation of fluorescent ATP analog labeled with Cy3. When 10 nM Cy3-ATP was applied to S-1 on the surface, the background fluorescence due to free Cy3-ATP was low, because the illumination region was localized near the quartz slide surface (Fig. 6A). When Cy3-ATP or -ADP was associated with surface-bound Cy5-S-1, which had been recorded previously (Fig. 6B), it could be seen as a clear, in-focus fluorescent spot (Fig. 6C); free Cy3-ATP undergoing rapid Brownian motion, on the other hand, was not seen as a discrete spot. Hence, by observing the presence and lifetime of stationary, in-focus Cy3 molecules corresponding to the positions of Cy5-S-1 molecules on the surface, we could detect individual association–

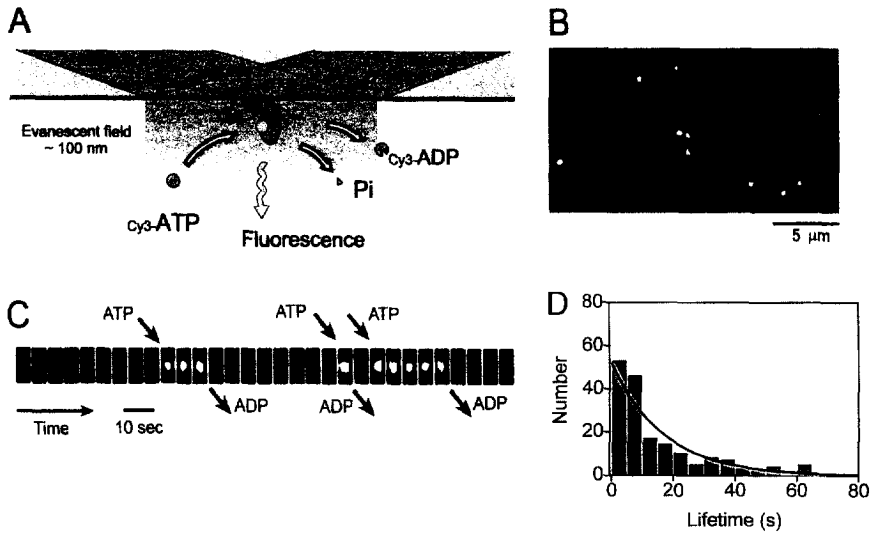

Fig. 6. Visualization of individual ATP turnovers by single S-1 molecules. (A) Schematic of the principle of measurement. (B) Fluorescence micrograph of single Cy5-labeled S-1 molecules bound to the surface. (C) ATP turnovers by a single S-1 molecule. Typical images of fluorescence from Cy3-nucleotide coming in and out of focus by associating with and dissociating from an S-1 indicated by the arrowhead in B. (D) Histogram of the lifetime of Cy3-nucleotides bound to S-1 molecules. The dissociation rate (1/lifetime) was determined to be 0.059 s^{-1} from the exponential fitting, which was consistent with the value of Mg-Cy3-ATPase rate of S-1 suspended in solution (0.045 s^{-1}).

(hydrolysis)–dissociation of Cy3-ATP with single S-1. Fig. 6C shows the association and dissociation of single Cy3-ATP/ADP molecules with a single S-1 molecule (indicated by an arrow head in Fig. 6B).

Fig. 6D shows the histogram of the lifetime of bound Cy3-ATP or -ADP which reveals an exponential dissociation rate $k_{-} = 0.059\,s^{-1}$. The photobleaching of Cy3-ATP hardly affects the results as its lifetime (1/photobleaching rate), when bound to a quartz surface, was ~ 85 s at the same laser power (3.8 mW). The Mg-Cy3-ATPase rate of S-1 suspended in solution was $0.045 \pm 0.002\,s^{-1}$ ($n = 2$), which was similar to that of the Mg-ATPase rate ($0.063 \pm 0.001\,s^{-1}$, $n = 3$). The dissociation rate is in good agreement with the ATP turnover rate of Cy3-ATP by S-1 suspended in solution ($0.045 \pm 0.002\,s^{-1}$), suggesting that the binding and dissociation of Cy3-ATP/ADP visualized by microscopy is a single ATP turnover. Since individual S-1 molecules could turn over Cy3-ATP during several minutes of observation, illumination of Cy3-nucleotide bound to S-1 does not appear to diminish enzymatic activity.

3.4. Individual ATP turnovers by single kinesin molecules captured by optical tweezers

TIRFM for single molecule imaging was combined with the technique of optical tweezers (Fig. 7).

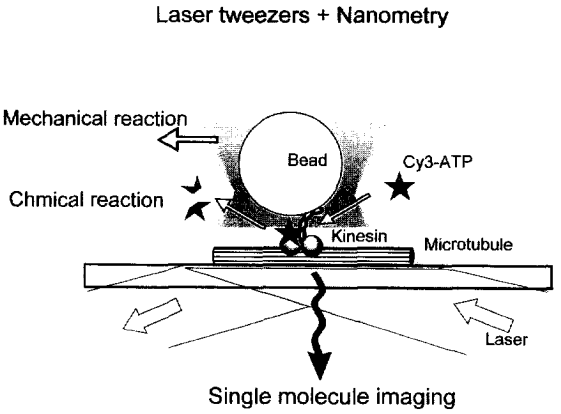

Fig. 7. Schematic drawing of the measurements of the mechanical elementary events and individual ATP turnovers by single kinesin molecules. Three optics for single molecule imaging, optical tweezers and nanometer sensing are combined.

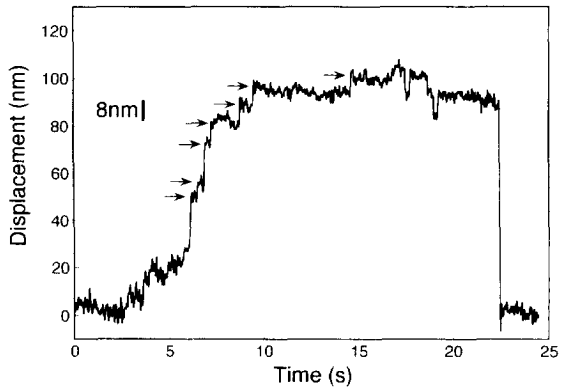

Fig. 8. Displacement of a bead caused by a single kinesin in the presence of 4 μM of Cy3-ATP were detected by the system shown in Fig. 7. Mechanical elementary events, i.e. 8 nm steps by a single kinesin molecule, are shown by arrows.

A single kinesin molecule was attached to a polystyrene bead trapped by an infrared laser [22]. By controlling the position of a bead with the optical tweezers, the kinesin molecule was brought into contact with a microtubule adsorbed onto the glass surface. A nanometer sensor [6,8,22] was installed in the present system to measure the elemental mechanical events, i.e. 8 nm steps of a single kinesin molecule [22]. In the previous experiment, Cy3-ATP was derivatized through the N^6-position of the adenine ring. In this experiment, we used Cy3-ATP derivatized through the ribose, because it is superior in promoting motile activity of motor protein. Ribose-linked Cy3-ATP was found to be a good ATP analog and 8 nm steps taken by kinesin in the presence of Cy3-ATP were clearly detected, as shown in Fig. 8. The individual ATP turnovers by kinesin were measured by counting the number of photons from Cy3-ATP attached to kinesin. To improve temporal resolution to the order of milliseconds, a photon counting device was used instead of a video camera at the image plane. Fig. 9 shows the time course of the fluorescence intensities from Cy3-ATP or -ADP bound to the kinesin. The frequency of turnover events was rather small, because the concentration of Cy3-ATP added was as low as 50 nM to reduce background fluorescence from free Cy3-ATP. The lifetime of bound Cy3-ATP or -ADP in the absence of microtubule was 10 s. It was greatly shortened to 0.08 s when kinesin was brought into contact with a microtubule. Since the lifetime of

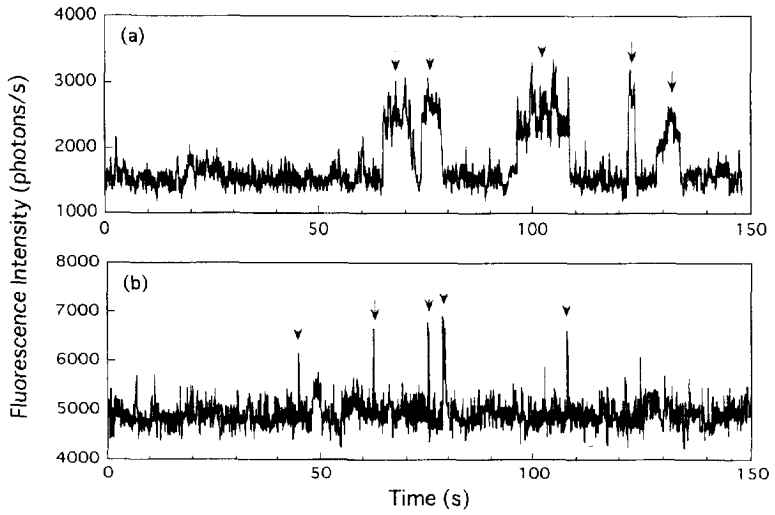

Fig. 9. Cy3-ATP turnovers by a kinesin molecule in the absence of a microtubule (a) or by a kinesin molecule interacting with a microtubule (b). Photon currents from the Cy3-nucleotides attached to a kinesin were measured by an avalanche photodiode every 4 ms. The concentration of Cy3-ATP was 20 nM (a) and 50 nM (b), respectively.

bound nucleotides is nearly equal to the ATP turnover time at saturating ATP concentration, the results show that the ATPase activity of the kinesin is greatly activated by the microtubule as it is in solution [32–35].

It is now possible to measure simultaneously the individual ATP turnovers and elementary mechanical events of a single kinesin molecule [36]. This should provide a clear answer to the fundamental problem of how the mechanical reaction is coupled to the ATPase reaction.

4. Perspective

The technique for visualizing single molecules and its combination with nano-manipulation presented here could be widely used to measure motions and chemical reactions of biological systems such as DNA motors, ion pumps and ATP synthase at a single molecular level. It is possible to suspend a single DNA in solution with dual optical tweezers and also to see single fluorescently labeled RNA polymerases. Direct observation of the transcription of DNA by a single RNA polymerase molecule is now achievable. Furthermore, the technique of single molecule imaging enables imaging of fluorescence resonance energy transfer between a single donor and a single acceptor molecule bound to biomolecule(s). The fluorescence spectroscopy of single molecules in solution is now also available. These techniques will enable us to determine conformational states of individual protein molecules, and to follow the protein folding process, protein–protein or protein–ligand interaction at a single molecular level. Thus, the techniques for single molecule imaging and manipulation will most likely be very powerful for studies not only on motility of motor proteins but also on molecular genetics, signal transduction and processing in cell.

Acknowledgements

We thank Drs. T. Yagi for the preparation of axonemes, E. Muto for the single molecule fluorescence assay of kinesin, C. Coppin for critical reading of this manuscript, and colleagues of the ERATO project for valuable discussions.

References

[1] T. Yanagida, M. Nakase, K. Nishiyama, F. Oosawa, Nature 307 (1984) 58–60.

[2] S.J. Kron, J.A. Spudich, Proc. Natl. Acad. Sci. USA 83 (1986) 6272–6276.
[3] Y.Y. Toyoshima, S.J. Kron, E.M. McNally, K.R. Niebling, C. Toyoshima, J.A. Spudich, Nature 328 (1987) 536–539.
[4] Y. Harada, A. Noguchi, A. Kishino, T. Yanagida, Nature 326 (1987) 805–808.
[5] A. Kishino, T. Yanagida, Nature 334 (1988) 74–76.
[6] A. Ishijima, T. Doi, K. Sakurada, T. Yanagida, Nature 352 (1991) 301–306.
[7] A. Ishijima, Y. Harada, H. Kojima, T. Funatsu, H. Higuchi, T. Yanagida, Biochem. Biophys. Res. Commun. 199 (1994) 1057–1063.
[8] J.T. Finer, R.M. Simmons, J.A. Spudich, Nature 368 (1994) 113–119.
[9] Y. Harada, T. Yanagida, Cell Motil. Cytoskel. 10 (1988) 71–76.
[10] E. Betzig, R.J. Chichester, Science 262 (1993) 1422–1425.
[11] J.K. Trautman, J.J. Macklin, E. Betzig, Nature 369 (1994) 40–42.
[12] T. Funatsu, Y. Harada, M. Tokunaga, K. Saito, T. Yanagida, Nature 374 (1995) 555–559.
[13] D. Axelrod, Methods Cell Biol. 30 (1989) 245–247.
[14] P.L. Southwick, L.A. Ernst, E.W. Tauriello, S.R. Parker, R.B. Mujumdar, S.R. Mujumdar, H.A. Clever, A.S. Waggoner, Cytometry 11 (1990) 418–430.
[15] F. Navone, J. Niclas, N. Hom-Booher, L. Sparks, H.D. Bernstein, G. McCaffrey, R.D. Vale, J. Cell Biol. 117 (1992) 1263–1275.
[16] S. Itakura, H. Yamakawa, Y.Y. Toyoshima, A. Ishijima, T. Kojima, Y. Harada, T. Yanagida, T. Wakabayashi, K. Sutoh, Biochem. Biophys. Res. Commun. 196 (1993) 1504–1510.
[17] R. Kamiya, E. Kurimoto, E. Muto, J. Cell Biol. 112 (1991) 441–447.
[18] Y. Harada, K. Sakurada, T. Aoki, D.D. Thomas, T. Yanagida, J. Mol. Biol. 216 (1990) 49–68.
[19] S. Lowey, G.S. Waller, M.K. Trybus, Nature 365 (1993) 454–456.
[20] M. Lindberg, K. Mosbach, Eur. J. Biochem. 53 (1975) 481–486.
[21] T. Kodama, K. Fukui, K. Kometani, J. Biochem. (Tokyo) 99 (1986) 1465–1472.
[22] K. Svoboda, C.F. Schmidt, B.J. Schnapp, S.M. Block, Nature 365 (1993) 721–727.
[23] B.J. Schnapp, T.S. Reese, Proc. Natl. Acad. Sci. USA 86 (1989) 1548–1552.
[24] K. Svoboda, S.M. Block, Cell 77 (1994) 773–784.
[25] L.T. Haimo, R.D. Fenton, Cell Motil. Cytoskel. 9 (1988) 129–139.
[26] A.D. Hyman, D. Drechsel, D. Kellogg, S. Salser, K. Sawin, P. Steffen, L. Wordeman, T. Mitchison, Methods Enzymol. 196 (1991) 478–485.
[27] C.R. Cremo, J.M. Neuron, R.G. Yount, Biochemistry 29 (1990) 3309–3319.
[28] A.J. Sowerby, C.K. Seehra, M. Lee, C.R. Bagshaw, J. Mol. Biol. 234 (1993) 114–123.
[29] I. Sase, H. Miyata, J.E.T. Corrie, J.S. Craik, K. Kinosita Jr, Biophys. J. 69 (1995) 323–328.
[30] R.D. Vale, T. Funatsu, D.W. Pierce, L. Romberg, Y. Harada, T. Yanagida, Nature 380 (1996) 451–453.
[31] S.M. Block, L.S. Goldstein, B.J. Schnapp, Nature 348 (1990) 348–352.
[32] D.D. Hackney, Proc. Natl. Acad. Sci. USA 85 (1988) 6314–6318.
[33] S.P. Gilbert, K.A. Johnson, Biochemistry 33 (1994) 1951–1960.
[34] Y.Z. Ma, E.W. Taylor, Biochemistry 34 (1995) 13242–13251.
[35] A. Lockhart, R.A. Cross, D.F.A. McKillop, FEBS Lett. 368 (1995) 531–535.
[36] T. Funatsu, Y. Harada, H. Higuchi, M. Tokunaga, K. Saito, R.D. Vale, T. Yanagida, Biophys. J. 70 (1996) A6.